

Thermozymes

Synthetic RNA thermometers based on ribozyme activity

Athanasios Saragliadis,¹ Stefanie S. Krajewski,² Charlotte Rehm,¹ Franz Narberhaus² and Jörg S. Hartig^{1,*}

¹Department of Chemistry and Konstanz Research School Chemical Biology (KoRS-CB); University of Konstanz; Konstanz, Germany; ²Microbial Biology; Ruhr University Bochum; Bochum, Germany

Keywords: gene expression, regulatory RNA, riboswitch, hammerhead ribozyme, RNA thermometer, temperature

Abbreviations: HHR, hammerhead ribozyme; RNAT, RNA thermometer; UTR, untranslated region; SD, shine-dalgarno; RBS, ribosome-binding site

Synthetic biology approaches often combine natural building blocks to generate new cellular activities. Here, we make use of two RNA elements to design a regulatory device with novel functionality. The system is based on a hammerhead ribozyme (HHR) that cleaves itself to generate a liberated ribosome-binding site and, thus, permits expression of a downstream gene. We connected a temperature-responsive RNA hairpin to the HHR and, thus, generated a temperature-controlled ribozyme that we call thermozyme. Specifically, a *Salmonella* RNA thermometer (RNAT) known to modulate small heat shock gene expression by temperature-controlled base-pairing and melting was fused to the ribozyme. Following an in vivo screening approach, we isolated two functional thermozymes. In vivo expression studies and in vitro structure probing experiments support a mechanism in which rising temperatures melt the thermometer structure impairing the self-cleavage reaction of the ribozyme. Since RNA cleavage is necessary to liberate the RBS, these engineered thermozymes shut off gene expression in response to a temperature increase and, thus, act in a reverse manner as the natural RNAT. Our results clearly emphasize the highly modular nature and biotechnological potential of ribozyme-based RNA thermometers.

Introduction

Gene expression is often regulated in response to variations of environmental parameters such as changing nutrient availability or altered physical conditions. Particularly in bacteria, regulatory RNAs are frequently involved in natural mechanisms of conditional gene expression.^{1,2} For example, riboswitches are RNA-based regulatory elements that are positioned in the 5'-untranslated region (5'-UTR) of the transcript they regulate.³⁻⁵ They are composed of an aptamer domain displaying high affinity and specificity for a cognate ligand. Usually, a second domain termed expression platform is located downstream of the aptamer domain. Upon ligand binding to the aptamer domain, a conformational change results in the formation of alternate folds in the expression platform that either change transcription termination or translation initiation.⁶⁻⁸ Following early proof of concept work,⁹ the discovery of naturally occurring RNA-based switches of gene expression has sparked a series of studies demonstrating the construction of synthetic riboswitches.^{10,11} The incorporation of in vitro-selected aptamers into mRNAs resulted in genetic switches in bacteria as well as eukaryotic organisms.^{12,13} More specifically, we and others have designed artificial riboswitches based on a ligand-dependent regulation of a self-cleaving hammerhead ribozyme.^{11,14-16} Although ligand-dependent ribozymes

have been developed even before the discovery of widespread use of riboswitch mechanisms in nature,¹⁷ such aptazymes have been applied in vivo for gene-regulatory purposes only after the discovery of catalytically well-behaved, fast-cleaving variants of the hammerhead ribozyme comprising stem I/II interactions.¹⁸⁻²⁰ In our opinion, ribozyme-based devices have the advantage of almost universal applicability for controlling RNA functions. Apart from regulating mRNA translation in bacteria and mRNA integrity in mammalian cells,^{21,22} they can be utilized in order to control the activity of tRNAs,²³ 16S rRNA,²⁴ as well as RNAi in mammalia.²¹ In addition, they can be combined in a modular fashion in order to yield two-input Boolean logic operators.²⁵

In addition to small molecule-responsive RNA sensors, gene expression can be controlled by temperature-sensitive RNA structures, so-called RNA thermometers (RNATs).²⁶ All known RNATs modulate translation efficiency by temperature-responsive RNA structures. Most of them function in a zipper-like manner by sequestering the Shine-Dalgarno (SD, part of the ribosome-binding site) sequence at low temperatures, hence inhibiting translation initiation.²⁷ At elevated temperatures, the secondary structure unfolds and liberates the SD sequence allowing translation of the downstream gene (Fig. 1A). Typical RNAT-controlled genes are either heat shock genes²⁸⁻³¹ or virulence genes.^{32,33} FourU-type RNAT control both classes of

*Correspondence to: Jörg S. Hartig; Email: joerg.hartig@uni-konstanz.de
Submitted: 03/18/13; Accepted: 03/28/13
<http://dx.doi.org/10.4161/rna.24482>

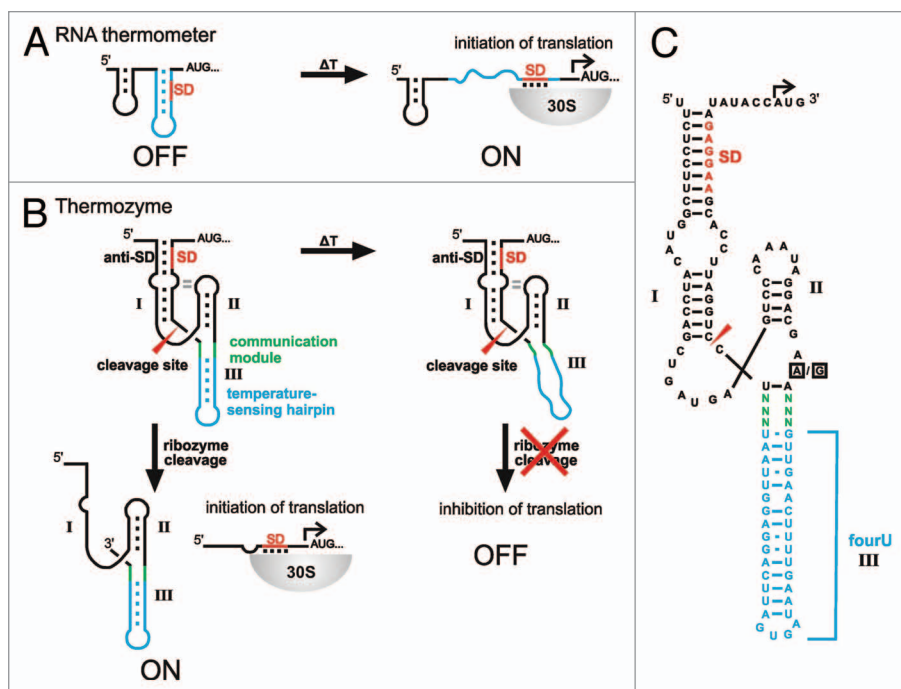


Figure 1. Design and mechanism of artificial HHR-based RNA thermometers. (A) General mechanism of naturally occurring RNA thermometers. A hairpin structure (blue) masks the Shine-Dalgarno sequence (SD; red) at low temperatures. Upon increased temperatures, melting of the secondary structure liberates the SD and translation is turned ON. 30S, small ribosomal subunit. (B) General design of a HHR-based RNA thermometer (Thermozyme). A temperature-sensing hairpin (blue) is fused via a communication module (green) to a hammerhead ribozyme with an extended stem I masking the SD (red). At low temperatures, the secondary structure permits the self-cleaving reaction of the ribozyme, liberating its SD and allowing translation of a downstream gene. A temperature increase results in melting of the thermosensing hairpin, thereby preventing self-cleavage and translation is shut OFF. Stems are indicated with roman numbers; the ribozyme cleavage site is marked by a red arrowhead. (C) Detailed thermozyme sequence. Stem III of the *Schistosoma mansoni* hammerhead ribozyme is exchanged against the temperature-sensing second hairpin of the *Salmonella agsA* thermometer (fourU hairpin). Red, SD of the downstream open reading frame; blue, temperature-sensing fourU hairpin; green, randomized nucleotides of the communication module; boxed nucleotides, ribozyme-inactivating point mutation (A→G).

genes.^{32,34} They are characterized by four uridines that mask the SD sequence at low temperatures. The best studied example is located in the 5'-UTR of the *Salmonella enterica* small heat shock gene *agsA*.³⁴ The second of two short hairpins, referred to as fourU hairpin in the remainder of this article, pairs with the SD sequence and regulates expression by heat-induced zipper-like melting.^{35,36} Based on the simple melting principle, artificial RNATs comprised of one or two stem-loop structures have been designed.^{37,38} Entirely unrelated elements with RNAT-like behavior are four-stranded G-rich sequences capable of forming RNA quadruplex structures in *Escherichia coli*. Potential quadruplex sequences were positioned in a way that formation of the quadruplex structure resulted in masking of the SD sequence. Thermal destabilization of that structure resulted in increased gene expression.³⁹

All currently known natural and synthetic RNAT control translation initiation. Therefore, we asked whether RNATs controlling other biological processes can be designed. Here, we exploit the simplicity of the *Salmonella* fourU hairpin to design

HHR-based RNAT (thermozymes). Previously, we achieved ligand-dependency of artificial gene switches by attaching an theophylline aptamer to stem III of the ribozyme.¹⁵ Screening for optimized linker sequences is often required to facilitate communication between ligand binding and ribozyme activity. In this study, we used the *Salmonella* fourU stem-loop as a building block to implement temperature sensitivity into an RNA-based device for artificial temperature control of gene expression. The constructed HHR-based RNATs respond to increased temperatures by an initial melting of the temperature-sensitive hairpin while the overall structure stays intact (Fig. 1B). With our design, artificial RNA thermosensors are obtained, which show a temperature-dependency inverse to the parental, naturally occurring thermometers.

Results

Construction of Thermozymes. In order to construct a synthetic HHR-based RNAT, we attached the thermosensitive fourU hairpin to the ribozyme in place of stem III of a parental HHR derived from *Schistosoma mansoni* (SC-HHR), see Figure 2A. The position was chosen in order to preserve stem I/II interactions that facilitate fast cleavage kinetics at physiological Mg^{2+} concentrations in naturally occurring HHRs.^{18–20} To screen for sequences that respond to changing temperatures with altered gene expres-

sion, we randomized six nucleotides (Fig. 1C, communication module highlighted in green) located at the junction between the ribozyme core and the fourU hairpin. A pool of different clones was constructed by inserting the randomized ribozyme sequences upstream of the eGFP gene for efficient in vivo screening. Single clones were isolated and screened for temperature responsiveness. For this purpose, the bacteria were grown at 20°C and 37°C followed by determination of gene expression by fluorescence measurements. The strain harboring the eGFP plasmid showed significant increase in gene expression at 37°C compared with growth at 20°C and the parental HHR control construct (SC-HHR) harboring the constitutively active variant of the ribozyme showed slightly increased eGFP expression at 37°C (Fig. 2C). In the screening procedure, we identified two clones with significantly higher eGFP expression at lower temperatures as compared with 37°C (Fig. 2B). At 20°C, the two constructs F1-HHR and B6-HHR exhibited a 3.5-fold and 3-fold induction of gene expression compared with expression at 37°C (Fig. 2C). Normalized to the expression values of

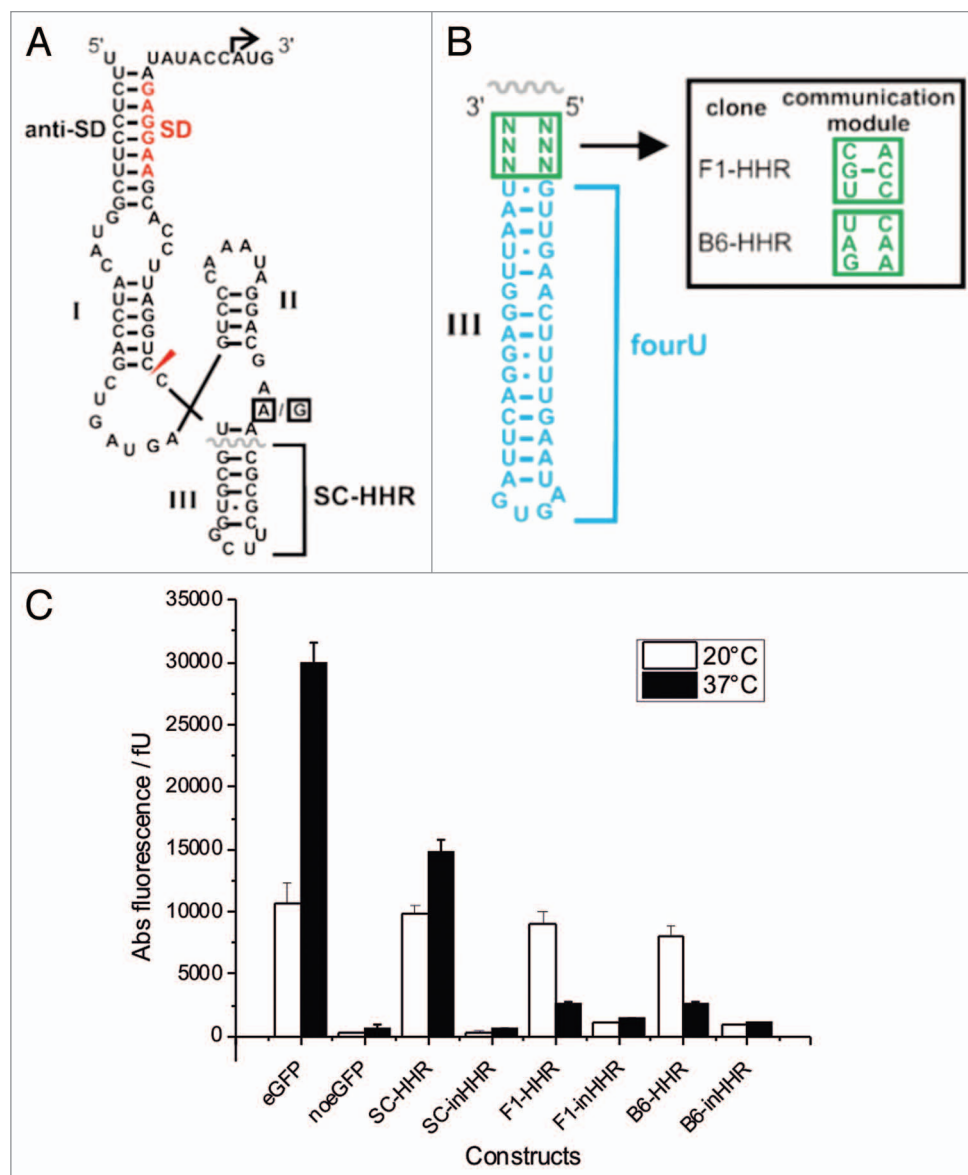


Figure 2. Characteristics of functional temperature-responsive ribozyme switches. (A) Sequence and secondary structure of the parental, constitutively active construct SC-HHR containing a stable, short stem-loop in position III of the HHR. The boxed nucleotides in the catalytic core mark the position of the inactivating point mutation (A→G). (B) Sequence of the fourU hairpin attached to stem III of the HHR, boxed square, randomized positions for the screening procedure. Inset shows screened sequences of communication modules of the two temperature-responsive clones F1-HHR and B6-HHR. (C) In vivo expression levels of various HHR constructs controlling the eGFP gene in *E. coli*: white bars, 20°C; black bars, 37°C. inHHRs represent catalytically inactive variants generated by the point mutation marked by boxed nucleotides in 2A.

the parental SC-HHR construct, the changes of gene expression amount to 5.2-fold and 4.5-fold for clones F1-HHR and B6-HHR, respectively.

In order to validate that the observed regulation of gene expression is based on the self-cleavage reaction of the ribozymes, we introduced an inactivating A→G point mutation (Fig. 1C) in the catalytic core of the ribozyme, yielding the two inhibited constructs F1-inHHR and B6-inHHR. As expected, gene expression was impaired because translation initiation requires ribozyme activity (Fig. 1B) and was not temperature-controlled anymore (Fig. 2C). This finding indicates that ribozyme activity is necessary for gene expression to occur.

In vitro characterization of Thermozyms. In order to characterize whether gene regulation in vivo indeed occurs via the anticipated mechanism of stem III destabilization upon increased temperature and subsequent ribozyme inactivation, we determined the temperature-dependent in vitro cleavage kinetics of the F1-HHR candidate compared with the constitutively active control ribozyme SC-HHR. The ribozyme constructs were in vitro transcribed using T7 RNA polymerase from a synthetic DNA template spanning the 5'-end of the mRNA until the end of the SD sequence, complementing stem I of the ribozyme. To prevent autocatalytic cleavage of the HHRs during transcription, we added a blocking strand at high concentrations that hybridizes

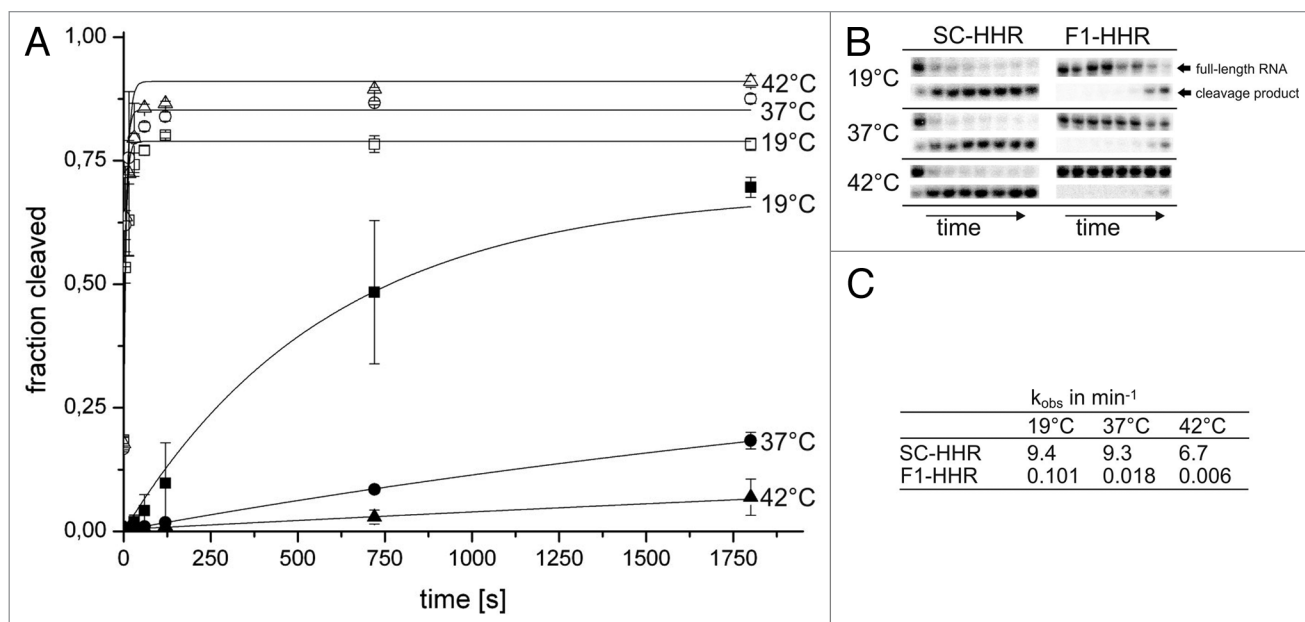


Figure 3. Cleavage kinetics of in vitro-transcribed, purified hammerhead ribozyme variants. (A) Time course of ribozyme cleavage reactions. (SC-HHR 19°C open squares, SC-HHR 37°C open circle, SC-HHR 42°C open triangle, F1-HHR 19°C black square, F1-HHR 37°C black circle, F1-HHR 42°C black triangle). Reactions were performed using 100 nM ribozyme and were initiated with 0.5 mM MgCl₂. Samples were taken at 0, 5, 15, 30, 60, 120, 720, 1,800 sec, analyzed by denaturing PAGE and band intensities were quantified. Errors have been calculated from three independent experiments. (B) PAGE-analysis of cleavage reactions. Parts of the gel corresponding to the full-length RNA and 5' cleavage product are shown. (C) k_{obs} values (min⁻¹) determined for the SC-HHR and the F1-HHR at different temperatures.

to the catalytic core of the HHR and was removed during subsequent gel purification.⁴⁰ Ribozyme reactions were started by addition of MgCl₂ to a final concentration of 0.5 mM at 19°C, 37°C and 42°C. The constitutively active SC-HHR construct containing a stable stem III shows very fast cleavage kinetics at 19°C and 37°C with only a slight decrease at 42°C (Fig. 3A and B). After 5 sec, the majority of the full-length ribozyme RNA was cleaved (Fig. 3B). For the SC-HHR variant cleavage rates of 9.4–6.7 min⁻¹ were calculated (Fig. 3C). These values compare well to kinetics of fast-cleaving variants at sub-millimolar Mg²⁺-concentrations.¹⁶ In contrast to SC-HHR, cleavage of the thermozyme F1-HHR was considerably slower at all temperatures (Fig. 3C). More importantly, the cleavage rate significantly decreased with increasing temperatures (more than 16-fold from 19°C to 42°C, see Fig. 3C). This temperature-dependent behavior is in accordance with the observed gene regulation in vivo.

In order to demonstrate temperature-controlled melting of stem III as basis for the thermozyme action, we performed structure-probing experiments of in vitro-transcribed HHR constructs. To prevent self-cleavage of the ribozymes prior to and during the probing procedure, we analyzed the variants SC-inHHR and F1-inHHR inactivated by the A→G point mutation in the catalytic core of the ribozyme. In general, probing with nucleases S1, V1 and T1 resulted in a cleavage pattern consistent with the predicted secondary structures of the HHRs (Fig. 4). RNase S1 is known to cleave single-stranded regions, whereas V1 is specific for double-stranded and stacked regions. T1 preferentially cleaves 3' of single-stranded guanines. The SC-inHHR construct containing a stable stem III structure shows basically the same

cleavage pattern at both 25°C and 42°C (Fig. 4A). For example, G residues in stem III did not become accessible to RNase T1 at 42°C. In contrast, construct F1-inHHR shows significant changes in RNase susceptibility at different temperatures (Fig. 4B). At low temperatures the overall structure is comparable to the structure of SC-inHHR while at higher temperatures cleavage of hairpin III resembled that of the original *Salmonella agsA* thermometer.³⁴ More specifically, the thermosensing fourU structure was protected from RNase S1 and T1 cleavage at 25°C, while nucleotides in this region were readily cleaved at 42°C.

Fine-mapping of Thermozyme structures. In order to further characterize specific melting of the thermosensitive fourU hairpin, we performed enzymatic cleavage in a temperature range from 20–45°C. The cleavage pattern for construct F1-inHHR shows that the nucleotides of the thermosensing hairpin III are accessible for RNase S1 cleavage at higher temperature indicating melting of the hairpin (Fig. 5A and C). In addition to structural changes in the RNAT module, the catalytic core and parts of stem II also showed partial melting at elevated temperatures, consistent with inactivation of ribozyme catalysis. To address whether the second thermozyme candidate B6-HHR behaves like F1-HHR, we compared the temperature-dependent structural alterations of B6-inHHR with F1-inHHR. Both showed a similar melting profile regardless of the different communication modules (Fig. 5B and C).

Discussion

Temperature-responsive HHRs were constructed by the fusion of a temperature-labile hairpin originating from a natural RNA

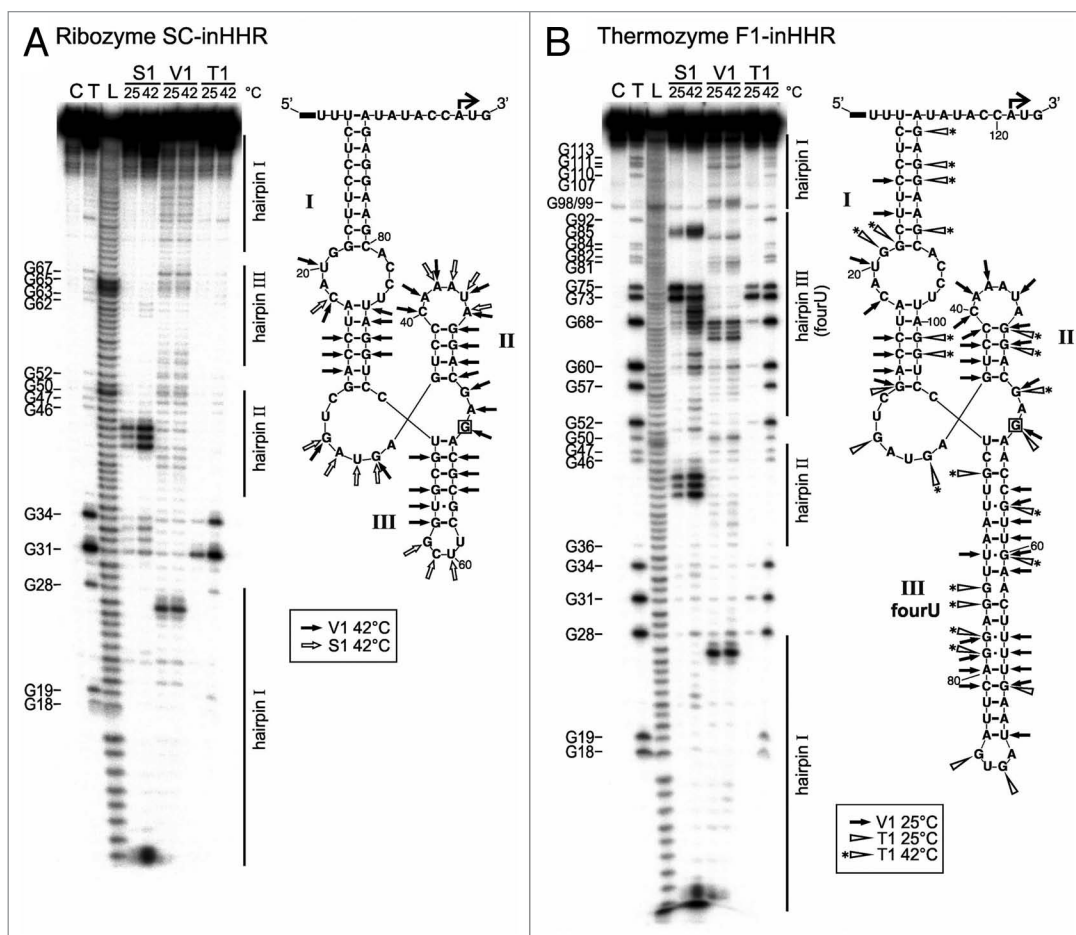


Figure 4. Structural analysis of the inactive hammerhead ribozyme SC-inHHR and the inactive thermozyme variant F1-inHHR. Enzymatic cleavage of 5' end-labeled RNA was performed with nuclease S1 (0.25 U), RNase V1 [0.002 U (A) or 0.004 U (B)] and RNase T1 (0.005 U) at 25 and 42°C. RNA fragments were separated on an 8% polyacrylamide gel. Lane C, RNA treated with water instead of RNase served as control; lane T, RNase T1 cleavage at 50°C; lane L, alkaline ladder. (A) Structure probing of the inactive ribozyme SC-inHHR (left) and secondary structure model with probing results at 42°C (right). Boxed nucleotide: position of the inactivating mutation of the HHR (A→G). Cleavage sites introduced at 42°C by nuclease S1 and RNase V1 are indicated by arrows. (B) Structure probing of the inactive thermozyme F1-inHHR (left) and secondary structure model with probing results (right). Boxed nucleotide: position of the inactivating mutation of the HHR (A→G). Cleavage sites introduced by RNase T1 and RNase V1 at 25°C are indicated by arrows. Additionally, RNase T1 cleavage sites at 42°C are marked by arrows with asterisks.

thermometer to a self-cleaving hammerhead ribozyme. By screening for optimized sequences, two thermozymes were obtained that act as inverted, artificial RNATs when utilized as control elements for gene expression within a 5'-UTR of an *E. coli* mRNA. So far, aptamers binding several ligands were combined with HHRs functioning as expression platforms in order to control mRNAs, tRNAs, 16S rRNA as well as RNAi in organisms as diverse as bacteria and mammalian cells.^{11,15,16,21,23-25,41}

The present work shows that a physical stimulus such as a change in temperature can also be used in order to regulate gene expression via a hammerhead-mediated mRNA cleavage reaction. Importantly, most natural RNAT and all previously engineered RNAT are composed of secondary structures that mask the SD sequence.^{37,38} At elevated temperatures, gene expression is turned on by increased ribosome binding due to a more accessible, single-stranded SD region. In contrast, melting of the same thermo-sensitive structure in our artificial HHR design results in slowing down ribozyme cleavage rates, which, in turn, results in

inhibition of gene expression since the HHR itself masks the SD region in the non-cleaved state. In conclusion, our design allows the construction of artificial RNA thermosensors with inversed temperature behaviors.

Modular RNA-based building blocks might be useful for future applications within the field of synthetic biology since they represent gene regulatory elements that do not require protein cofactors. Even simpler, there is also no need for externally added ligands in order to control gene expression. In addition to the potential applications of such artificial gene control devices in synthetic biology and biotechnology, the presented work demonstrates that a temperature-sensitive fourU hairpin adopted from the *Salmonella agsA* gene can be used as a modular component in combination with other functional RNA units. Although some other parts such as the catalytic core and stem II of the ribozyme are destabilized as well, the fourU structure melts rather specifically at increased temperatures and, thus, provides a basis for rendering the HHR temperature-responsive.

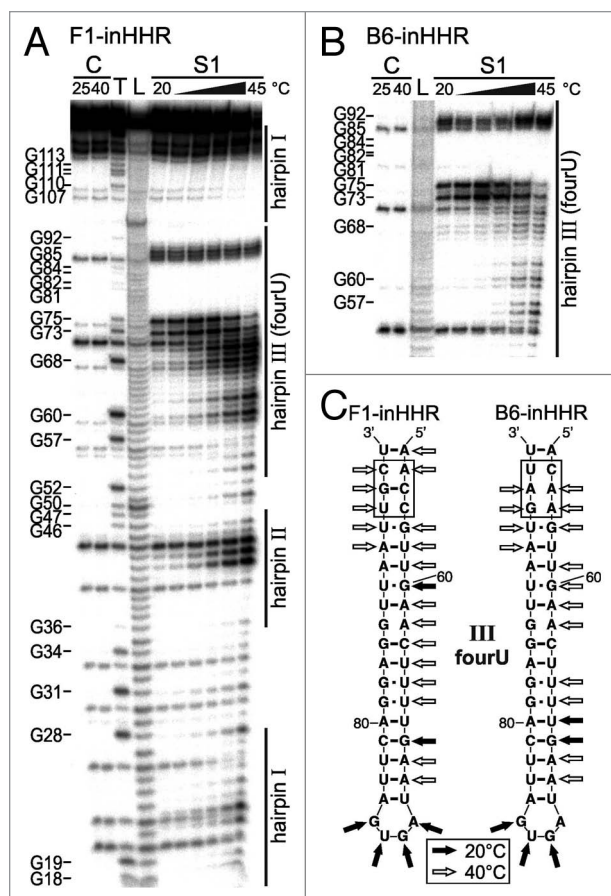


Figure 5. Temperature-dependent alterations of the inactive thermozymes F1-inHHR and B6-inHHR. Enzymatic cleavage of 5' end-labeled RNAs with RNase S1 (0.25 U) was performed in a temperature range from 20–45°C in intervals of 5°C. RNA fragments were separated on an 8% polyacrylamide gel. Lane C, RNA treated with water instead of RNase at the indicated temperatures served as control; lane T, RNase T1 cleavage at 50°C; lane L, alkaline ladder. **(A)** Fine-mapping of the inactive thermozyme variant F1-inHHR. **(B)** Fine-mapping of the inactive thermozyme variant B6-inHHR. Detail of the gel corresponding to hairpin III (fourU hairpin) of the thermozyme is shown. **(C)** Structure model of the thermosensing hairpins III of both thermozyme variants with results of the enzymatic probing. Cleavage sites introduced by RNase S1 at 20 and 40°C are indicated by arrows. The communication modules are marked by boxes.

The possibility to confer temperature regulation to a ribozyme both in vivo and in vitro by fusion with a natural RNAT hairpin emphasizes the remarkable modular nature of functional RNA motifs.

Materials and Methods

Plasmid construction. All constructs were introduced into a plasmid harboring the parental HHR derived from *Schistosoma mansoni* (SC-HHR) (HHR_{pET16b-eGFP})¹⁵ by PCR using Phusion DNA Polymerase (Finzyme) and sequence-specific primers with the designed construct sequences attached to the 5' end of the primers. The following primers were used:

Pet16b_RBS_hp2_Fw: CTATTCAAAAAGTTCACAN
 NNTTTCGTCCTATTTGGGACTCATCAGC

Pet16b_RBS_hp2_Rv: TGATTTCAGGAGGTTAATN
 NNTCCTGGATTCCACGAAGGAGATATACC

N represents an unbiased random position generated during solid phase DNA synthesis using a 1:1:1:1 mixture of nucleoside phosphoramidites. Following the PCR, the template plasmid was digested with DpnI. The PCR products were ligated (Quick Ligase, NEB) and afterwards transformed into *E. coli* BL21(DE3) gold (Stratagene). Single colonies were picked and grown in LB-Medium supplemented with 100 µgml⁻¹ carbenicilline (Roth). To confirm successful cloning, the cloned plasmids were isolated (Miniprep Kit, Qiagen) and sequenced.

In vivo screening for functional Thermozymes. For identifying temperature-responsive HHR constructs, single clones of the transformed thermosensor-HHR pool were picked into 96 deep well plates. The expression of eGFP of out-grown cultures at room temperature and at 37°C was compared. In detail *E. coli* cells [BL21 (DE3), Stratagene] harboring the various plasmids were grown in Luria-Bertani (LB) medium with carbenicillin (100 µgml⁻¹) at 37°C under continuous shaking (1,050 r.p.m.). After 24 h, bacteria were diluted in fresh medium in a 96 deep well format and grown at room temperature under continuous shaking (1,050 r.p.m) for 2 d. After the first 24 h, 1 µl of the cell culture at room temperature was used to inoculate fresh medium in a 96 deep well format and grown at 37°C under continuous shaking (1,050 r.p.m) for 24 h, hence obtaining two cell cultures (one at room temperature and one at 37°C) after further 24 h. Two hundred µL of each culture were transferred into 96-well

microplates and the fluorescence of the expressed eGFP was measured with a plate reader, using excitation wavelength of 488 nm and emission wavelength of 533 nm. The measured fluorescence was normalized to the cell optical density, measured at 600 nm.

Ribozyme kinetics. For in vitro transcription of ribozymes, a T7 RNA polymerase promoter was attached to the 5'-end of the ribozyme sequences. Synthetic DNA templates of SC-HHR and F1-HHR were PCR amplified using primers and templates shown in Table 1. The PCR products were purified by ethanol precipitation and subsequently in vitro transcribed using T7 RNA polymerase (Fermentas) in Transcription Buffer (40 mM TRIS-HCl pH 7.9, 6 mM MgCl₂, 10 mM DTT, 10 mM NaCl, 2 mM spermidine, 0.5 mM ATP, 2 mM CTP, 2 mM GTP and 2 mM UTP) and 1 µCi ³²P-α-ATP. One hundred µM blocking strand (ATT TGG GAC TCA TCA GCT GG) was added to the reaction mixture to prevent autocatalytic cleavage of the ribozymes during transcription. In vitro transcription was performed at 37°C for 2 h and subsequently purified by ethanol precipitation. The pellet was solved in 80 µL 0.5x stop buffer [40% (v/v) formamide, 25 mM EDTA pH 8.0, 0.012% (w/v) bromphenolblue]. The RNA was purified on an 8% denaturing PAGE. Full-length products were excised and passively eluted from the gel. RNA concentrations were determined photometrically.

For the determination of ribozyme activities, 100 nM of ribozyme in 50 mM TRIS-HCl pH 7.5, 100 mM KCl were heated to 94°C for 2 min and then slowly cooled to 19°C to fold the ribozyme. The mixtures were then incubated at 19°C, 37°C or 42°C and the cleavage reaction was started by addition of Mg²⁺ to

Table 1. Primers, templates and 5'-UTR sequences of ribozymes and thermozyms utilized in this study

Name	Sequence
fw-Primer	GAA ATT AAT ACG ACT CAC TAT AGG GAG TCT CCT TCG GTA CAT CCA GCT GAT GAG TCC CAA ATA GGA CGA AA
rev-Primer	TCT CCT TCG TGG AAT CCA GG
Template: SC-HHR	ATG AGT CCC AAA TAG GAC GAA ACG CGC TTC GGT GCG TCC TGG ATT CCA CGA AGG AGA-3'
Template: F1-HHR	ATG AGT CCC AAA TAG GAC GAA AAC CGT TGA ACT TTT GAA TAG TGA TTC AGG AGG TTA ATT GCT CCT GGA TTC CAC GAA GGA GA
5'-UTR: F1-HHR	AUU CCC CUU <u>UCU CCU UCG</u> GUA CAU CCA GCU GAU GAG UCC CAA AUA GGA CGA AAA CCG <u>UUG AAC UUU UGA AUA GUG AUU CAG GAG</u> <u>GUU AAU UGC UCC UGG AUU CCA CGA AGG AGA UAU ACC AUG...</u>
5'-UTR: F1-inHHR	AUU CCC CUU <u>UCU CCU UCG</u> GUA CAU CCA GCU GAU GAG UCC CAA AUA GGA CGA g AA CCG <u>UUG AAC UUU UGA AUA GUG AUU CAG GAG</u> <u>GUU AAU UGC UCC UGG AUU CCA CGA AGG AGA UAU ACC AUG...</u>
5'-UTR: B6-HHR	AUU CCC CUU <u>UCU CCU UCG</u> GUA CAU CCA GCU GAU GAG UCC CAA AUA GGA CGA AAC AAG <u>UUG AAC UUU UGA AUA GUG AUU CAG GAG</u> <u>GUU AAU GAU UCC UGG AUU CCA CGA AGG AGA UAU ACC AUG...</u>
5'-UTR: B6-inHHR	AUU CCC CUU <u>UCU CCU UCG</u> GUA CAU CCA GCU GAU GAG UCC CAA AUA GGA CGA g AC AAG <u>UUG AAC UUU UGA AUA GUG AUU CAG GAG</u> <u>GUU AAU GAU UCC UGG AUU CCA CGA AGG AGA UAU ACC AUG...</u>
5'-UTR: SC-HHR	AUU CCC CUU <u>UCU CCU UCG</u> GUA CAU CCA GCU GAU GAG UCC CAA AUA GGA CGA AAC GCG CUU CGG UGC GUC CUG GAU UCC ACG <u>AAG</u> <u>GAG AUA UAC CAU G...</u>
5'-UTR: SC-inHHR	AUU CCC CUU <u>UCU CCU UCG</u> GUA CAU CCA GCU GAU GAG UCC CAA AUA GGA CGA g AC GCG CUU CGG UGC GUC CUG GAU UCC ACG <u>AAG</u> <u>GAG AUA UAC CAU G...</u>

Constructs are shown up to the start codon of eGFP. SD (5'-AAGGAG-3') and anti-SD region are underlined. HHR region is indicated in italics. fourU hairpin is double underlined. Bold lower case letters indicate an A→G point mutation resulting in an inactive ribozyme.

a final concentration as indicated. Samples were taken at defined time points and the reactions were quenched by addition of 1x stop buffer. The reaction mixtures were separated on an 8% denaturing PAGE and visualized by phosphorimaging. To determine the cleavage rates k_{obs} , the data was fitted using the equation:

$$F_t = F_{max} - (F_{max} - F_0) \times e^{-k_{obs}t}$$

F_t , fraction cleaved at time t ; F_{max} , maximal fraction cleaved; F_0 , fraction cleaved before the reaction was started.

Enzymatic probing of Thermozyne structures. For the generation of run-off plasmids, a fragment carrying the ribozyme sequences with the T7 promoter sequence at the 5'-end and an EcoRV restriction site at the 3'-end was amplified with the primers runoff_fw (5'-AGAAATTAATACGACTCACTA TAGGGATTCCCCCTTTCTCCTTCGGTA-3') and runoff_rv (5'-TTGATATCCATGGTATATCTCCTTCGT GG-3') and cloned into the SmaI site of pUC18. SC-inHHR, F1-inHHR and B6-inHHR RNAs were synthesized in vitro by run-off transcription with T7 RNA polymerase from EcoRV-linearized

plasmids. Partial digestions of 5'-³²P-labeled RNA with ribonucleases T1 (Ambion), V1 (Ambion) and nuclease S1 (Fermentas, ThermoScientific) were conducted according to reference 34 with the exception that 1 μ l of 5x TN buffer for RNase T1 (100 mM TRIS-acetate, pH 7.5; 500 mM NaCl), 1 μ l of 10x RNA structure buffer for RNase V1 (provided with RNase) or 1 μ l 5x reaction buffer for nuclease S1 (provided with nuclease) were used per reaction. The alkaline ladder was generated as described previously.⁴²

Disclosure of Potential Conflicts of Interest

No potential conflicts of interest were disclosed.

Acknowledgments

We thank Astrid Joachimi and Cornelius Kullmann for assistance. This work was supported by a Lichtenberg Professorship awarded to J.S.H. by the *VolkswagenStiftung*, and by a grant of the German Research Foundation (DFG, SPP 1258: Sensory and regulatory RNAs in Prokaryotes) to F.N.

References

- Scott WG, Martick M, Chi YI. Structure and function of regulatory RNA elements: ribozymes that regulate gene expression. *Biochim Biophys Acta* 2009; 1789:634-41; PMID:19781673; <http://dx.doi.org/10.1016/j.bbarm.2009.09.006>.
- Ying SY, Chang DC, Lin SL. The microRNA (miRNA): overview of the RNA genes that modulate gene function. *Mol Biotechnol* 2008; 38:257-68; PMID:17999201; <http://dx.doi.org/10.1007/s12033-007-9013-8>.
- Barrick JE, Corbino KA, Winkler WC, Nahvi A, Mandal M, Collins J, et al. New RNA motifs suggest an expanded scope for riboswitches in bacterial genetic control. *Proc Natl Acad Sci USA* 2004; 101:6421-6; PMID:15096624; <http://dx.doi.org/10.1073/pnas.0308014101>.
- Roth A, Breaker RR. The structural and functional diversity of metabolite-binding riboswitches. *Annu Rev Biochem* 2009; 78:305-34; PMID:19298181; <http://dx.doi.org/10.1146/annurev.biochem.78.070507.135656>.
- Winkler WC, Breaker RR. Regulation of bacterial gene expression by riboswitches. *Annu Rev Microbiol* 2005; 59:487-517; PMID:16153177; <http://dx.doi.org/10.1146/annurev.micro.59.030804.121336>.
- Breaker RR. Prospects for riboswitch discovery and analysis. *Mol Cell* 2011; 43:867-79; PMID:21925376; <http://dx.doi.org/10.1016/j.molcel.2011.08.024>.
- Winkler W, Nahvi A, Breaker RR. Thiamine derivatives bind messenger RNAs directly to regulate bacterial gene expression. *Nature* 2002; 419:952-6; PMID:12410317; <http://dx.doi.org/10.1038/nature01145>.
- Winkler WC, Cohen-Chalamish S, Breaker RR. An mRNA structure that controls gene expression by binding FMN. *Proc Natl Acad Sci USA* 2002; 99:15908-13; PMID:12456892; <http://dx.doi.org/10.1073/pnas.212628899>.

9. Werstuck G, Green MR. Controlling gene expression in living cells through small molecule-RNA interactions. *Science* 1998; 282:296-8; PMID:9765156; <http://dx.doi.org/10.1126/science.282.5387.296>.
10. Suess B, Weigand JE. Engineered riboswitches: overview, problems and trends. *RNA Biol* 2008; 5:24-9; PMID:18388492; <http://dx.doi.org/10.4161/rna.5.1.5955>.
11. Wieland M, Hartig JS. Artificial riboswitches: synthetic mRNA-based regulators of gene expression. *Chembiochem* 2008; 9:1873-8; PMID:18604832; <http://dx.doi.org/10.1002/cbic.200800154>.
12. Hanson S, Berthelot K, Fink B, McCarthy JE, Suess B. Tetracycline-aptamer-mediated translational regulation in yeast. *Mol Microbiol* 2003; 49:1627-37; PMID:12950926; <http://dx.doi.org/10.1046/j.1365-2958.2003.03656.x>.
13. Weigand JE, Sanchez M, Gunnesch EB, Zeiher S, Schroeder R, Suess B. Screening for engineered neomycin riboswitches that control translation initiation. *RNA* 2008; 14:89-97; PMID:18000033; <http://dx.doi.org/10.1261/rna.772408>.
14. Wieland M, Hartig JS. Investigation of mRNA quadruplex formation in *Escherichia coli*. *Nat Protoc* 2009; 4:1632-40; PMID:19876023; <http://dx.doi.org/10.1038/nprot.2009.111>.
15. Wieland M, Hartig JS. Improved aptazyme design and in vivo screening enable riboswitching in bacteria. *Angew Chem Int Ed Engl* 2008; 47:2604-7; PMID:18270990; <http://dx.doi.org/10.1002/anie.200703700>.
16. Wieland M, Gfell M, Hartig JS. Expanded hammerhead ribozymes containing addressable three-way junctions. *RNA* 2009; 15:968-76; PMID:19304923; <http://dx.doi.org/10.1261/rna.1220309>.
17. Soukup GA, Breaker RR. Engineering precision RNA molecular switches. *Proc Natl Acad Sci USA* 1999; 96:3584-9; PMID:10097080; <http://dx.doi.org/10.1073/pnas.96.7.3584>.
18. Khvorova A, Lescoute A, Westhof E, Jayasena SD. Sequence elements outside the hammerhead ribozyme catalytic core enable intracellular activity. *Nat Struct Biol* 2003; 10:708-12; PMID:12881719; <http://dx.doi.org/10.1038/nsb959>.
19. Martick M, Scott WG. Tertiary contacts distant from the active site prime a ribozyme for catalysis. *Cell* 2006; 126:309-20; PMID:16859740; <http://dx.doi.org/10.1016/j.cell.2006.06.036>.
20. De la Peña M, Gago S, Flores R. Peripheral regions of natural hammerhead ribozymes greatly increase their self-cleavage activity. *EMBO J* 2003; 22:5561-70; PMID:14532128; <http://dx.doi.org/10.1093/emboj/cdg530>.
21. Ausländer S, Ketzner P, Hartig JS. A ligand-dependent hammerhead ribozyme switch for controlling mammalian gene expression. *Mol Biosyst* 2010; 6:807-14; PMID:20567766; <http://dx.doi.org/10.1039/b923076a>.
22. Ketzner P, Haas SF, Engelhardt S, Hartig JS, Nettelbeck DM. Synthetic riboswitches for external regulation of genes transferred by replication-deficient and oncolytic adenoviruses. *Nucleic Acids Res* 2012; 40:e167; PMID:22885302; <http://dx.doi.org/10.1093/nar/gks734>.
23. Berschneider B, Wieland M, Rubini M, Hartig JS. Small-molecule-dependent regulation of transfer RNA in bacteria. *Angew Chem Int Ed Engl* 2009; 48:7564-7; PMID:19739151; <http://dx.doi.org/10.1002/anie.200900851>.
24. Wieland M, Berschneider B, Erlacher MD, Hartig JS. Aptazyme-mediated regulation of 16S ribosomal RNA. *Chem Biol* 2010; 17:236-42; PMID:20338515; <http://dx.doi.org/10.1016/j.chembiol.2010.02.012>.
25. Klausner B, Saraglidis A, Ausländer S, Wieland M, Berthold MR, Hartig JS. Post-transcriptional Boolean computation by combining aptazymes controlling mRNA translation initiation and tRNA activation. *Mol Biosyst* 2012; 8:2242-8; PMID:22777205; <http://dx.doi.org/10.1039/c2mb25091h>.
26. Storz G. An RNA thermometer. *Genes Dev* 1999; 13:633-6; PMID:10090718; <http://dx.doi.org/10.1101/gad.13.6.633>.
27. Kortmann J, Narberhaus F. Bacterial RNA thermometers: molecular zippers and switches. *Nat Rev Microbiol* 2012; 10:255-65; PMID:22421878; <http://dx.doi.org/10.1038/nrmicro2730>.
28. Kortmann J, Szodrok S, Rinnenthal J, Schwalbe H, Narberhaus F. Translation on demand by a simple RNA-based thermosensor. *Nucleic Acids Res* 2011; 39:2855-68; PMID:21131278; <http://dx.doi.org/10.1093/nar/gkq1252>.
29. Morita MT, Tanaka Y, Kodama TS, Kyogoku Y, Yanagi H, Yura T. Translational induction of heat shock transcription factor sigma32: evidence for a built-in RNA thermosensor. *Genes Dev* 1999; 13:655-65; PMID:10090722; <http://dx.doi.org/10.1101/gad.13.6.655>.
30. Nocker A, Hausherr T, Balsiger S, Krstulovic NP, Hennecke H, Narberhaus F. A mRNA-based thermosensor controls expression of rhizobial heat shock genes. *Nucleic Acids Res* 2001; 29:4800-7; PMID:11726689; <http://dx.doi.org/10.1093/nar/29.23.4800>.
31. Waldminghaus T, Fippinger A, Alfsmann J, Narberhaus F. RNA thermometers are common in alpha- and gamma-proteobacteria. *Biol Chem* 2005; 386:1279-86; PMID:16336122; <http://dx.doi.org/10.1515/BC.2005.145>.
32. Böhme K, Steinmann R, Kortmann J, Seekircher S, Heroven AK, Berger E, et al. Concerted actions of a thermo-labile regulator and a unique intergenic RNA thermosensor control *Yersinia* virulence. *PLoS Pathog* 2012; 8:e1002518; PMID:22359501; <http://dx.doi.org/10.1371/journal.ppat.1002518>.
33. Johansson J, Mandin P, Renzoni A, Chiaruttini C, Springer M, Cossart P. An RNA thermosensor controls expression of virulence genes in *Listeria monocytogenes*. *Cell* 2002; 110:551-61; PMID:12230973; [http://dx.doi.org/10.1016/S0092-8674\(02\)00905-4](http://dx.doi.org/10.1016/S0092-8674(02)00905-4).
34. Waldminghaus T, Heidrich N, Brantl S, Narberhaus F. FourU: a novel type of RNA thermometer in *Salmonella*. *Mol Microbiol* 2007; 65:413-24; PMID:17630972; <http://dx.doi.org/10.1111/j.1365-2958.2007.05794.x>.
35. Rinnenthal J, Klinkert B, Narberhaus F, Schwalbe H. Direct observation of the temperature-induced melting process of the *Salmonella* fourU RNA thermometer at base-pair resolution. *Nucleic Acids Res* 2010; 38:3834-47; PMID:20211842; <http://dx.doi.org/10.1093/nar/gkq124>.
36. Rinnenthal J, Klinkert B, Narberhaus F, Schwalbe H. Modulation of the stability of the *Salmonella* fourU-type RNA thermometer. *Nucleic Acids Res* 2011; 39:8258-70; PMID:21727085; <http://dx.doi.org/10.1093/nar/gkr314>.
37. Neupert J, Karcher D, Bock R. Design of simple synthetic RNA thermometers for temperature-controlled gene expression in *Escherichia coli*. *Nucleic Acids Res* 2008; 36:e124; PMID:18753148; <http://dx.doi.org/10.1093/nar/gkn545>.
38. Waldminghaus T, Kortmann J, Gesing S, Narberhaus F. Generation of synthetic RNA-based thermosensors. *Biol Chem* 2008; 389:1319-26; PMID:18713019; <http://dx.doi.org/10.1515/BC.2008.150>.
39. Wieland M, Hartig JS. RNA quadruplex-based modulation of gene expression. *Chem Biol* 2007; 14:757-63; PMID:17656312; <http://dx.doi.org/10.1016/j.chembiol.2007.06.005>.
40. Salehi-Ashtiani K, Szostak JW. In vitro evolution suggests multiple origins for the hammerhead ribozyme. *Nature* 2001; 414:82-4; PMID:11689947; <http://dx.doi.org/10.1038/35102081>.
41. Kumar D, An CI, Yokobayashi Y. Conditional RNA interference mediated by allosteric ribozyme. *J Am Chem Soc* 2009; 131:13906-7; PMID:19788322; <http://dx.doi.org/10.1021/ja905596t>.
42. Brantl S, Wagner EG. Antisense RNA-mediated transcriptional attenuation occurs faster than stable antisense/target RNA pairing: an in vitro study of plasmid pIP501. *EMBO J* 1994; 13:3599-607; PMID:7520390.